

SIMULATION AND SHOT-BY-SHOT MONITORING OF LINAC BEAM HALO*

Alan S. Fisher[†], Mei Bai, Thomas Frosio, Alessandro Ratti, John Smedley, Juhao Wu
SLAC National Accelerator Laboratory, Menlo Park, California, USA
Isar Mostafanezhad and Ben Rotter, Nalu Scientific, Honolulu, Hawaii, USA

Abstract

FELs require a reproducible distribution of the bunch core at the undulator entrance for robust and reliable lasing. However, various mechanisms drive particles from the core to form a beam halo, which can scrape the beam pipe of the undulator and damage its magnets. Collimators can trim the halo, but at the 1-MHz repetition rate of SLAC's LCLS-II superconducting linac, the collimator jaws can be activated and damaged. The Machine Protection System (MPS) can detect excessive radiation and halt the beam, but repeated MPS trips lead to significant downtime. Halo control begins by studying its structure, formation, and evolution, using a sensitive halo monitor. To that end, we are developing a pixellated diamond sensor. Diamond offers a dynamic range of up to 7 orders of magnitude, extending from the edge of the core to the faint halo expected at greater distances. Nalu Scientific has developed fast electronics for high-rate shot-by-shot readout. Initial tests are starting with a prototype 16-pixel sensor at the beam dump of SLAC's FACET-II test facility. The tests and simulations will guide more elaborate sensor designs.

INTRODUCTION

Generating a beam with the desired particle distribution in the core of each bunch and maintaining this distribution as the beam travels is a critical requirement for accelerators. However, various mechanisms drive particles from the core into a beam halo. At x-ray free-electron laser (XFEL) facilities, the shape of the bunch core at the entrance of the undulator is crucial for lasing. Reproducibility of this shape is necessary for robust and reliable performance. If a halo surrounds the core, it could scrape on the undulator beam pipe, generating a radiation shower that damages the undulator's permanent magnets. Our numerical simulation of LCLS-II with a start-to-end electron beam-dynamics model finds that collective effects will cause an electron beam—4 GeV, repeating at 300 kHz, 180 pC, plus both dark current and halo electrons—to scrape 1 to 10 W at the undulator entrance. Collimators are commonly used to trim the halo, but at the 1-MHz repetition rate of LCLS-II, the resulting radiation could activate and damage the collimator jaws, making this approach problematic. Moreover, the Machine Protection System (MPS) detects excessive radiation and halts the beam, but repeated MPS trips creates significant downtime for users.

Advanced techniques to detect and mitigate halo are necessary. Non-destructive characterization of the halo

distribution is crucial for understanding in detail the mechanisms behind its formation and for identifying countermeasures. We are developing pixellated diamond sensors surrounding the beam core, to monitor halo noninvasively (“parasitically”), shot by shot, with high spatial and temporal resolution. Diamond offers several orders of magnitude of dynamic range, allowing measurements from the edge of the core to the faint halo expected at greater distances. Below we describe an initial test using a diamond chip with 16 pixels, by the beam dump of FACET-II [1], the test-beam facility at SLAC. Fast electronics built by Nalu Scientific [2] provide shot-by-shot pixel readout.

PIXELLATED DIAMOND DETECTORS

Diamond Sensors

The diamond sensor used in this monitor is based on more than a decade of experience using diamond as an x-ray beam diagnostic [3-5]. In effect, these devices form a solid-state ionization chamber: a photon or electron excites an energetic electron within the material, which then loses energy via electron-electron scattering, producing one electron-hole pair for each 13.3 eV [6] of deposited energy. The FACET electron beam is near the minimum of the dE/dx curve, with an expected collisional energy loss of 35 keV/electron for a 50- μm -thick diamond. With the current electronics, we anticipate being sensitive to 10 electrons per pixel.

These devices have demonstrated a linear dynamic range spanning 11 orders of magnitude with photons [3, 4], due to the lack of recombination in the bulk, and are very radiation tolerant. We anticipate at least 7 orders of magnitude when used with electrons. The device can be read in pulsed or current mode. The goal is to resolve the halo in space—by dividing the chip's surface into pixels using lithographic patterning of the electrodes—and in time—by using pulse-mode readout for shot-by-shot data. In addition to its radiation hardness, diamond is an attractive medium for halo monitoring because its low Z makes it significantly less sensitive than other semiconductors to bremsstrahlung photons, which create background for direct halo detection.

Figure 1 shows the relatively simple patterned diamond in the FACET-II test. The chip is a square single crystal, 4 mm on each side and 50 μm -thick. Four parallel electrode strips, each platinum with a width of 750 μm and a thickness of 25 nm, cross one face with a 1-mm period. The second face has four similar strips, but orthogonal to those on the first. Their intersections form a 4 \times 4 grid of pixels. Figure 2 shows a microscope photograph of the diamond.

Future detectors are envisioned with many more pixels, spread over several chips. Each detector will surround the

* SLAC is supported by the U.S. Department of Energy, Office of Science, under contract DE-AC02-76SF00515.

[†] afisher@slac.stanford.edu

bunch core while remaining outside the beam stay-clear radius, to measure the halo noninvasively. A close approach to this radius will require a mechanical adjustment of the size of the central hole.

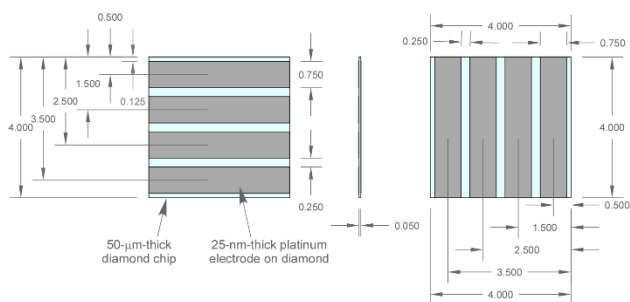


Figure 1: Pattern (in mm) of the platinum electrodes on both faces of the diamond chip.

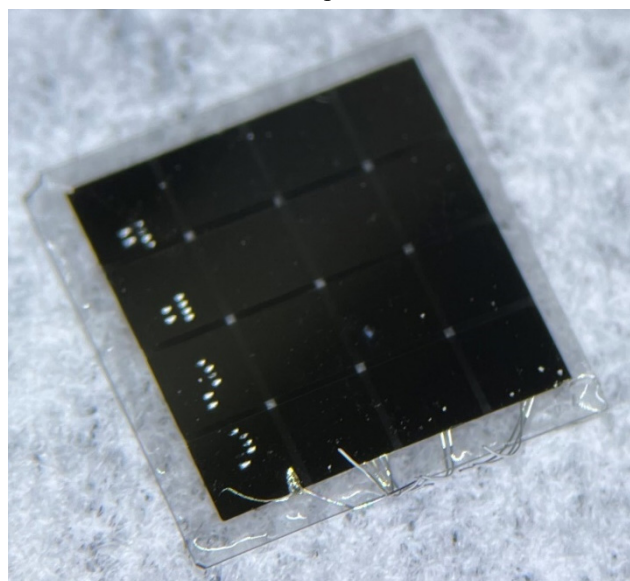


Figure 2: A microscope photo of the diamond. The diamond is clear. The electrodes, which appear black, on the upper surface run parallel to the lower edge. Those on the lower face can be seen through the gaps in the upper electrodes. Old wires from a previous bonding to the circuit board hang from the lower edge.

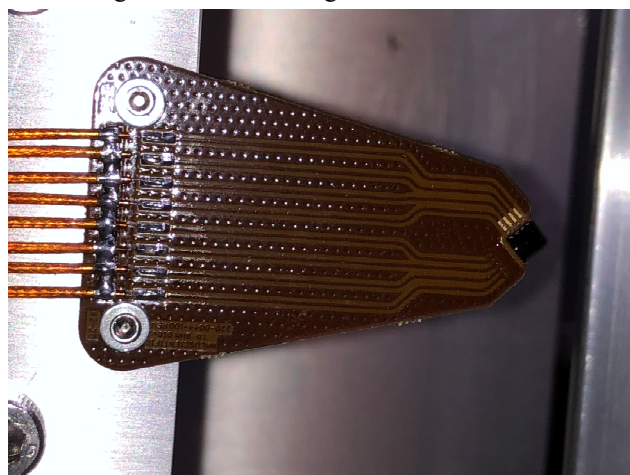


Figure 3: The diamond detector of Fig. 2, mounted on the printed circuit for fan-out to the 8 coaxial cables.

Shot-by-Shot Pixel Readout

The device tested at FACET-II evolved from the readout designed for a Time-Resolved Beam-Halo Monitor (TR-BHM) developed by Nalu Scientific in collaboration with another of the authors (J. Smedley).

The eight strips are wire bonded to a small printed-circuit board (Fig. 3) supporting the chip and fans out to eight coaxial cables running to a nearby amplifier box. Each channel is AC-coupled to the amplifier and DC coupled to a bias voltage. The DC supply is typically set to 30 V. The amplifier outputs are digitised in a separate module further from the beamline and transported over ethernet to a computer outside the tunnel. We use Nalu Scientific's AARD-VARC digitiser hardware [2] along with Nalu's *Naluscope* software for viewing and control.

Normally the strips on one side are grounded (for example, the horizontal strips, which correspond to the y coordinate) and those on the other are biased (vertical, giving the x coordinate). In a low-density halo, only one pixel may receive charge. This pixel is identified by the horizontal and vertical strips that receive nonzero signals. With a higher density, the bias is applied to only one strip of the four. Then the x coordinate is determined by the bias and the y profile comes from reading the charge on the grounded face. The bias is moved from strip to strip over four shots, giving the full pixel distribution. For an $N \times N$ grid, this method is a trade-off: N shots rather than one, but $2N$ cables and channels rather than N^2 . The advantage is less significant for our simple chip than for future devices.

HALO TEST AT FACET-II

FACET-II [1] is SLAC's test facility for advanced accelerator research, primarily studies of plasma-wakefield acceleration. The vertical bend at the beam dump serves as a spectrometer for the resulting wide changes in beam energy from an initial energy of typically 10 GeV. Electrons exit the beamline vacuum through a flange with a 5-mm-thick aluminium window and pass through more than 2 m of air while going over a diagnostics table and bending downward into the dump. This arrangement is convenient for a proof-of-principle test. It provides a first look at halo without the need for in-vacuum motion of the diamond sensor. After a long downtime, FACET-II is now being tuned, starting at the injector. The beam should be sent to the dump around the time of this conference. We anticipate beginning parasitic measurements shortly afterward.

The detector is mounted 185 cm from the window, at beam height and on a 50-mm horizontal translation stage. At one end of the travel, the beam core is roughly centred on the chip. We will begin with it fully retracted away from the beam. Then the signals from the chip will give an indication of the noise background, from the pulsed RF power and from the beam itself. This noise floor sets one end of the measurement's dynamic range. The beam can be stopped on a collimator just upstream to see the ambient electronic noise. The additional noise when the beam next goes to the dump will give the background due to the beam.

Content from this work may be used under the terms of the CC-BY-4.0 licence (© 2023). Any distribution of this work must maintain attribution to the author(s), title of the work, publisher, and DOI

We will then translate the diamond slowly toward the beam while monitoring the signals. An increase should be seen once the beam enters the halo. This movement can be continued until the beam approaches within perhaps 2σ of the centre (where σ is the RMS beam size). The dump bend can scan the halo vertically to vary the signals as the dipole shifts beam above and below the detector. Small controlled horizontal moves can be made with a horizontal corrector. (With no readback other than a video image of the position, the translation stage is imprecise for horizontal scanning.) The signals must be carefully watched near the core to avoid saturation. Damage to the simple FR4 circuit board is a concern if too much beam scatters from the diamond; a more expensive ceramic board will be needed in the next in-vacuum test (discussed below). The dynamic range extends at least between the highest level that seems safe and the noise floor.

Additional tests are needed to validate the halo measurement, since halo has an uncertain distribution that can extend to several times σ from the beam centre. The detector should appropriately register changes in the bunch size as the spectrometer quadrupoles change the focus. A suitable phase advance can image the collimator about 50 m upstream of the dump onto the detector. As the jaws are opened or closed, the moving image of the jaws should cut into the halo.

SIMULATION OF DIAMOND RESPONSE

We conducted a simulation to find the spread of the bunch after travel through the window and the air path, and the resulting charge deposition in the diamond. This study used a GEANT4 [7] model replicating the real geometry of the pixellated diamond detector (Fig. 4). The model integrates the intricate arrangement of strips and the diamond itself. Essential parameters such as particle position, direction, and energy entering the FACET-II exit flange are obtained from the ELEGANT beam-dynamics code [8]. Figure 5 (a) shows the transverse distribution at the exit window. The x and y projections, in Figs. 5(b) and (c) respectively, demonstrate that both distributions have long tails of halo electrons. The much lower density of the tails calls for a detector with a wide dynamic range, to record electrons in both the core and halo. The parameters are given to the GEANT4 simulation, which includes the exit window, the 185-cm air path to the diamond, and the detector itself.

Our simulation applies two distinct scoring approaches. The first is based on transfer functions provided by Cividec [9], a manufacturer of diamond detectors. These provide the interaction probabilities of various particle types within the diamond and the resulting charge generated, as a function of particle energy. The data accounts only for electrons, photons, protons, and neutrons. In the second scoring method, GEANT4 directly computes the energy deposition within the diamond, and an electron-hole pair is created for every 13.3 eV deposited [6].

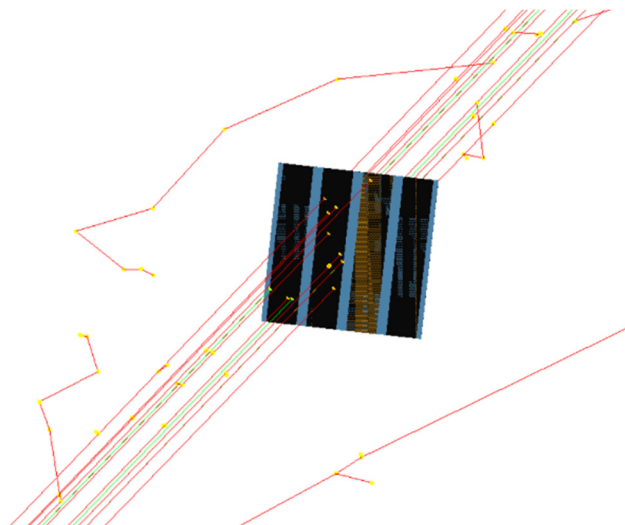


Figure 4: A GEANT4 simulation in which 10 primary 10-GeV electrons pass through the air path and the diamond detector. Electrons are shown in red and photons in green.

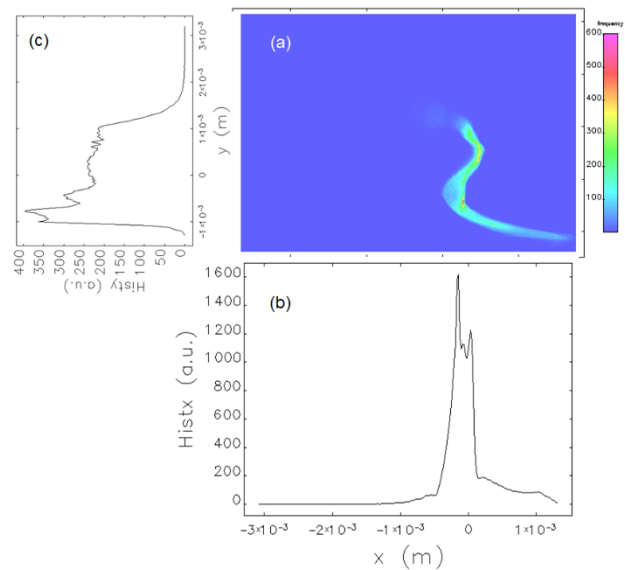


Figure 5: (a) Simulated transverse distribution of the electron bunch at the exit window, with projections along the (b) x and (c) y coordinates.

We find that these two methods agree both qualitatively and quantitatively. The spatial distribution of the diamond signals aligns well, while relative differences of 20% to 60% (Fig. 6) are observed between the two approaches. To ascertain whether these discrepancies are due to secondary particles beyond electrons, photons neutrons, and protons, we simulated the energy deposited by alpha particles, deuterons, pions, and ions produced by interactions with air. We find a negligible contribution from these secondaries to the total energy deposition within the diamond, less than 0.015%, with 0.01% originating from alpha particles. This correspondence suggests that the simulation captures the diamond detector's response, which we will benchmark with our upcoming measurements.

Content from this work may be used under the terms of the CC-BY-4.0 licence (© 2023). Any distribution of this work must maintain attribution to the author(s), title of the work, publisher, and DOI

CIVIDEC FUNCTIONS				EDEP FUNCTIONS				Relative difference			
5.9E-05	2.9E-02	4.0E-03	2.4E-05	1.0E-04	3.8E-02	5.3E-03	4.0E-05	40%	25%	24%	41%
1.2E-04	7.4E-02	8.5E-04	1.0E-05	1.9E-04	9.9E-02	1.2E-03	2.6E-05	36%	26%	28%	60%
1.9E-03	7.9E-02	6.6E-03	1.1E-05	2.6E-03	1.1E-01	9.0E-03	2.6E-05	28%	27%	27%	56%
2.7E-02	1.4E-02	5.9E-05	4.9E-06	3.7E-02	2.0E-02	9.5E-05	1.4E-05	27%	27%	38%	66%

Figure 6: Comparison of the GEANT4 simulation results for FACET-II using the two scoring methods, in fC per primary electron. Left: Cividec transfer functions. Centre: Energy deposition from GEANT4. Right: Relative difference.

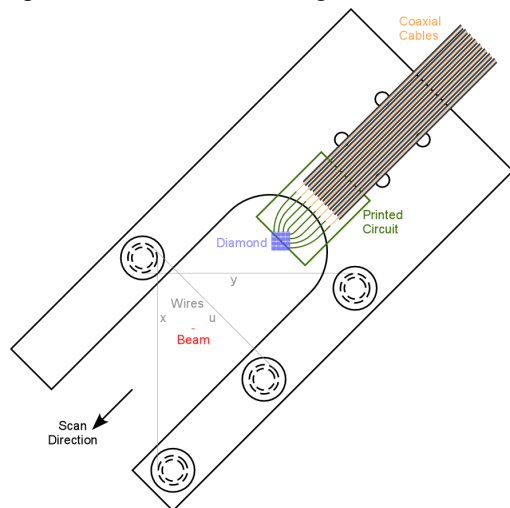


Figure 7: Sketch of a modified wire-scanner “harp”.

FUTURE WORK

FACET-II Measurement in Vacuum

As we begin the in-air measurements at the FACET-II beam dump, we are designing the next phase, a test in vacuum. To translate the detector from outside the beam into the halo, we will modify a surplus wire scanner. Minor changes to the “wire card” or “harp” that holds the wires will allow mounting the diamond on the moving stage (Fig. 7). The signals from the 8 strips will be connected through the vacuum in coaxial cables to a feedthrough flange for processing by Nalu’s electronics outside. The wire scanner allows us to measure the profile of the bunch core and the coordinates of its centroid relative to the diamond’s pixels. As the wire scanner moves the diamond through the halo, we will be able to map the halo over a region much larger than the size of the chip.

Halo Evolution

Effective halo mitigation must be guided by a better understanding of halo formation by interpreting measurements with simulations. These are also needed to guide the design of more advanced sensors, so that their extent and resolution can match the halo distribution at various locations along the FACET-II or LCLS-II beamlines. The complexities underlying beam halo are not yet well modelled and involve high-order nonlinear beam dynamics.

We plan to develop start-to-end particle-in-cell (PIC) numerical simulations of halo formation and evolution along the accelerator as extensions of various existing codes. Several well-benchmarked numerical simulation codes—including ASTRA, GPT, Elegant, Lucretia, and IMPACT—have been used successfully in designing and operating LCLS, LCLS-II, FACET and FACET-II, from electron-bunch generation through acceleration and bunch compression. These codes are well suited to form the basis for a model of beam halo.

However, due to the large extent of the beam’s distribution in 6-dimensional phase space, a high-order map for beam dynamics must be carefully implemented to model the generation and evolution of beam halo in the injector, accelerator, and bunch compressors. In particular, the core beam’s collective effects can drive the halo to execute betatron motion at large amplitude and with potentially significant chromatic effects. In the compressors, the model must incorporate 3-dimensional coherent synchrotron radiation (CSR) [10] to properly study transverse effects.

Understanding the formation and evolution of halo along the accelerator, through both measurement and simulation, will ultimately provide techniques for mitigating halo at its sources. These developments should prove valuable for LCLS and other XFELs.

REFERENCES

- [1] FACET-II Conceptual Design Report, SLAC, 2015.
- [2] L. Macchiarulo *et al.*, “Design improvements and first results for the revision 3 of AARDVARC Waveform Sampling System on Chip”, in *Proc. IEEE NSS-MIC 2020*, Boston, MA, USA (virtual), November 2020. doi:10.1109/NSS/MIC42677.2020.9507950
- [3] J. Bohon, E. Muller, J. Smedley, “Development of diamond-based X-ray detection for high-flux beamline diagnostics”, *J. Synchrotron Radiat.*, vol. 17, pp. 711-718, 2010. doi:10.1107/S0909049510031420
- [4] E. Muller *et al.*, “Transmission-mode diamond white-beam position monitor at NSLS”, *J. Synchrotron Radiat.*, vol. 19, pp. 381-387, 2012. doi:10.1107/S0909049512005043
- [5] T Zhou *et al.*, “Pixelated transmission-mode diamond X-ray detector”, *J. Synchrotron Radiat.*, vol. 22, pp. 1396-1402, 2015. doi:10.1107/S1600577515014824
- [6] J. Keister and J. Smedley, “Single Crystal Diamond Photodiode for Soft x-ray Radiometry”, *Nucl. Instrum. Methods A*, vol. 606, 774-779, 2009. doi:10.1016/j.nima.2009.04.044
- [7] S. Agostinelli *et al.*, “GEANT4—a simulation toolkit”, *Nucl. Instrum. Methods A*, vol. 506, pp. 250-303, 2003. doi:10.1016/S0168-9002(03)01368-8
- [8] M. Borland, “ELEGANT: A Flexible SDDS-Compliant Code for Accelerator Simulation”, Advanced Photon Source LS-287, September 2000.
- [9] E. Griesmayer, personal communication. <https://cividec.at>
- [10] Y. Cai and Y. Ding, “Three-dimensional Effects of Coherent Synchrotron Radiation by Electrons in a Bunch Compressor”, *Phys. Rev. Accel. Beams*, vol. 23, p. 014402, 2020. doi:10.1103/PhysRevAccelBeams.23.014402

Temporary page!

\LaTeX was unable to guess the total number of pages correctly. As there was some unprocessed data that should have been added to the final page this extra page has been added to receive it.

If you rerun the document (without altering it) this surplus page will go away, because \LaTeX now knows how many pages to expect for this document.